Fluorination and Electrical Conductivity of BN Nanotubes

7 AUTHORS, INCLUDING:

Yang Huang
Loughborough University

143 PUBLICATIONS **2,330** CITATIONS

Fangfang Xu
Chinese Academy of Sciences

52 PUBLICATIONS **1,505** CITATIONS

Dmitri Golberg
National Institute for Materials Science

643 PUBLICATIONS **22,665** CITATIONS

Fluorination and Electrical Conductivity of BN Nanotubes

Chengchun Tang,*,† Yoshio Bando,† Yang Huang,‡ Shuanglin Yue,‡ Changzhi Gu,‡
FangFang Xu,†,§ and Dmitri Golberg†

*Advanced Materials Laboratory, National Institute for Materials Science, Namiki 1-1, Tsukuba, Ibaraki 305-0044,
Japan, Beijing National Laboratory for Condensed Matter Physics, Institute of Physics, Chinese Academy of
Sciences, Beijing 100080, P. R. China, and Shanghai Institute of Ceramics, Shanghai 200050, P. R. China*

Received December 17, 2004; E-mail: tang.chengchun@nims.go.jp

The studies on BN nanotubes have been initiated due to the striking structural similarity between graphitic carbon and hexagonal BN.[1] The comparison between the two systems is of significant interest with respect to the development of functional nanomaterials and nanodevices. Due to the ionic origin of a BN band gap,[2] the electronic structure of BN nanotubes differs significantly from that of carbon nanotubes. Importantly, theoretical calculations[3] have demonstrated that BN nanotubes possess a very stable gap of ~5.5 eV, almost independent of tube diameter, helicity, and of whether a nanotube is single- or multiwalled. The electronic structure of doped BN nanotubes is primarily determined by the chemical composition.[4] Relative uniformity of electronic properties in the BN nanotubes, combined with its chemical inertness, may be the key advantage for the nanoelectronic applications. In fact, there is no need to control the diameter and helicity of BN-based nano-electronic devices, which is extremely difficult to fulfill in the case of carbon nanotubes.[5] In this context, the uniformly doped BN nanotubes obtained through chemical modification would be a prospective object for tailoring the electronic properties.

Previous studies on functionalization of BN nanotubes have mainly focused on the B−N−C system through the control of a C content.[6] However, the helicity influence on the band gap has still been in effect.[7] Recently, Han et al.[8] used a simple chemical route to coat BN nanotubes with a conductive stannic oxide for the sensor applications, although the tube surface has been affected only. This fact reflects the well-known chemical inertness and poor wetting of BN nanotubes. To obtain the entire doping or functionalization, a novel feasible strategy is required that relies on the simultaneous nanotube growth and introduction of foreign species during a single experiment run.

In this study, we selected fluorine-functionalized BN nanotubes in order to pursue applications in nanoelectronics. Fluorination is one of the most effective pathways to affect transport properties. Since fluorine is a highly electronegative element and has the excessive valence electrons compared to B and N, the functionalization should be easily performed and should reliably yield an n-type semiconductor. First, we examined the direct reaction between BN nanotubes and fluorine or hydrogen fluoride. Although we were able to obtain F doping of BN nanotubes via a long-time reaction at a low temperature, the fluorine atoms only attached to the nanotube surface. Most unfortunately, this attachment was considerably unstable. The doped fluorine escapes easily when the tube is exposed to air or under standard beam irradiation in the electron microscope.

In this communication, we describe a novel original route toward the synthesis of F-doped BN nanotubes through the introduction of F atoms at the stage of tube growth. Basic BN crystal was synthesized by means of a traditional chemical vapor deposition (CVD) from a BF_3/NH_3 mixture system. The following chemical reactions that have been commonly used in the fabrication of a BN film were involved:[9]

$$2BF_3 + 9NH_3 \rightarrow B_2(NH)_3 + 6NH_4F \qquad (1)$$

$$B_2(NH)_3 \rightarrow 2BN + NH_3 \qquad (2)$$

The reactions were carried out in a tubular reactor made of sintered BN. The reactor was placed inside a silica tube heated electrically. The reaction system was first heated to 925 °C in a nitrogen gas flow. BF_3 and NH_3 were then separately introduced into the tube and mixed in the hot reactor zone. In the present experimental runs, a significant modification to the traditional method has been adopted: a lump of $MgCl_2$ (~30 mg) was placed into the high-temperature area of the reactor, acting as a CVD substrate. The introduction of $MgCl_2$ is intended for the catalyzed nanotube growth, based on our previous experimental results that a magnesium-containing impurity could promote the one-dimensional growth.[10] The fluorination may be accomplished through the NH_4F reaction on the freshly grown BN nanotubes:

$$NH_4F \rightarrow F^- + H^+ + NH_3 \qquad (3)$$

After the synthesis over 1 h, a colorless wool-like layer, ~10 mg in weight, appeared on the surface of the slightly sintering lump.

X-ray diffraction analysis indicates that the starting $MgCl_2$ has fully been converted to MgF_2 after the reaction. The wool-like product is solely made of a hexagonal BN. The strong diffraction peak (002) locates at $d = 0.330$ nm, slightly smaller than the parameter of 0.333 nm of pure BN nanotubes. Due to the close electronegativity, the doped fluorine should preferentially occupy nitrogen positions. The observed ~1% lattice contraction relates to the smaller covalent radius (64 pm) of fluorine compared to the 70 pm of nitrogen. The covalent feature of the dopant was further confirmed by a Fourier transformation infrared spectrum. The spectrum shows a sharp absorption peak of the B−N−B out-of-plane bending vibration and an extremely broad peak of the in-plane B−N transverse vibration, indicating a highly disordered atom arrangement in the hexagonal BN layers. Additional peaks located approximately at 930, 1020, 1670, and ~3200 cm^{-1} can be detected, peculiar to the primary vibrational features of a covalent B−F mode.[11]

Examinations by scanning electron microscopy (SEM) and transmission electron microscopy (TEM) indicate that the fluorine-doped BN crystals possess a nanotube-like morphology with considerably disordered walls, having a high aspect ratio with the lengths up to several micrometers and diameters of a few tens of nanometers (Figure 1a). High-resolution TEM images indicate that the disordered BN layers are composed of highly curled continuous BN sheets, suggesting that the six-numbered BN atomic rings within

† National Institute for Materials Science.
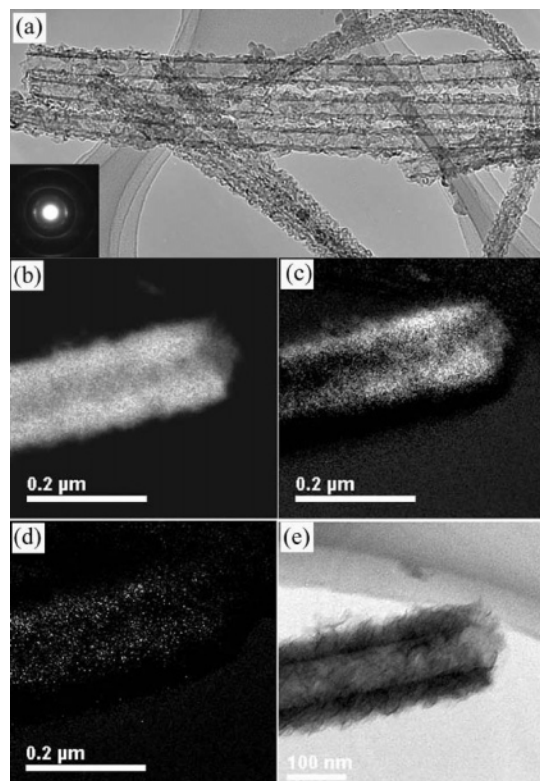‡ Chinese Academy of Sciences.
§ Shanghai Institute of Ceramics.

Figure 1. Low-magnification TEM image (a) and elemental maps of F-functionalized BN nanotubes synthesized using the BF_3/NH_3 system in the presence of $MgCl_2$ substrate: (b) B map; (c) N map; (d) F map, and (e) bright-field TEM image. Inset in (a): electron diffraction pattern taken from an individual tube, highlighting the disordered BN layer.

the BN sheets are strongly destroyed. This is quite different from the case of collapsed BN nanotubes when a six-membered ring structure is retained even under high temperature annealing in the presence of noble metals.[12] Energy-dispersion X-ray (EDX) analysis reveals that the elemental composition of BN_xF_y slightly changes from nanotube to nanotube, with statistic average values of $x \approx 0.97$ and $y \approx 0.07$. No traces of magnesium could be found. Electron energy loss spectra (EELS) of the sample reveal the B and N concentration as close to 1:1 stoichiometries and the F concentration of ~4 atom %. Considering the corresponding errors of EDX and EELS analyses, we would define the doping concentration as approximately 5%. We have also noticed that the concentration does not change when the sample is exposed to air or is electron-irradiated under TEM. The fluorine within the BN nanotubes is thus suggested to bond tightly. EELS mapping on the fluorinated BN nanotubes indicates the uniform fluorine distribution within the nanotubes. Representative elemental maps are shown in Figure 1b−e.

For the electrical measurements, we fabricated a standard four-terminal system (Figure 2a). The current−voltage ($I−V$) characteristics (Figure 2b) of an individual F−BN and an undoped and impurity-free BN nanotube may be compared; the latter has been synthesized by an in situ catalytic growth method.[10] The $I−V$ curve of the F−BN nanotube is nonlinear due to the Schottky barriers between the F−BN nanotube and the electrodes. The resistance of the F−BN nanotube is approximately $(2-4) \times 10^6$ Ω. Since the F−BN nanotube is <100 nm in diameter and ~5 μm in length, the resistivity of the individual F−BN is estimated as $0.2-0.6$ Ω·cm, indicating a typical heavy-doped semiconductor. For comparison, we also measured the $I−V$ characteristic of an individual pure BN nanotube using the same experimental setup. Shown in Figure 2b is the corresponding $I−V$ curve. It is symmetrical and linear
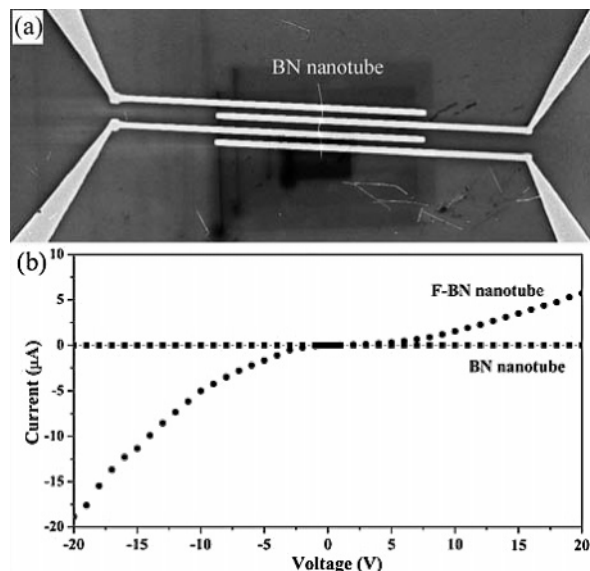

Figure 2. Four-probe measurement setup (a) for the comparative $I−V$ curve recording of a F-functionalized BN nanotube and an individual impurity-free BN nanotube (b).

due to the ohm contacts between the BN and electrode, and the currents are notably lower. In fact, the resistance and resistivity of the single BN nanotube are estimated as ~2×10^9 Ω and ~300 Ω·cm, respectively, which differ by 3 orders of magnitude compared to those of the doped BN nanotube.

In summary, fluorination of BN nanotubes results in highly curled tubular BN sheets and makes insulating BN nanotubes semiconducting. The phenomenon is assumed to be particularly important for the applications in the future nanoscale electronic devices with tunable properties.

Supporting Information Available: Experimental description, SEM images, XRD pattern, FTIR spectrum, high-resolution TEM image, and EELS and EDX spectra of the F−BN nanotubes (PDF). This material is available free of charge via the Internet at http://pubs.acs.org.

References

(1) (a) Terrones, M.; Hsu, W. K.; Terrones, H.; Zhang, J. P.; Ramos, S.; Hare, J. P.; Castillo, R.; Prassides, K.; Cheetham, A. K.; Kroto, H. W.; Walton, D. R. M. *Chem. Phys. Lett.* **1996**, *259*, 658. (b) Chopra, N. G.; Luyken, R. J.; Cherry, K.; Crespi, V. H.; Cohen, M. L.; Louie, S. G.; Zettl, A. *Science* **1995**, *269*, 966. (c) Loiseau, A.; Willaime, F.; Demoncy, N.; Hug, G.; Pascard, H. *Phys. Rev. Lett.* **1996**, *76*, 4737. (d) Golberg, D.; Bando, Y.; Eremets, M.; Takemura, K.; Kurashima, K.; Tamiya, K.; Yusa, H. *Chem. Phys. Lett.* **1997**, *279*, 191. (e) Deepak, F. L.; Vinod, C. P.; Mukhopadhyay, K.; Govindaraj, A.; Rao, C. N. R. *Chem. Phys. Lett.* **2002**, *353*, 345.
(2) Rubio, A.; Corkill, J. L.; Cohen, M. L. *Phys. Rev. B* **1994**, *49*, 5081.
(3) Blase, X.; Rubio, A.; Louie, S. G.; Cohen, M. L. *Europhys. Lett.* **1994**, *28*, 335.
(4) Blase, X.; Charlier, J. C.; De Vita, A.; Car, R. *Appl. Phys. Lett.* **1997**, *70*, 197.
(5) Crespi, V. H.; Cohen, M. L.; Rubio, A. *Phys. Rev. Lett.* **1997**, *79*, 2093.
(6) (a) Suenaga, K.; Colliex, C.; Demoncy, N.; Loiseau, A.; Pascard, H.; Willaime, F. *Science* **1997**, *278*, 653. (b) Mickelson, W.; Aloni, S.; Han, W. Q.; Cumings, J.; Zettl, A. *Science* **2003**, *300*, 467.
(7) Yoshioka, T.; Suzura, H.; Ando, T. *J. Phys. Soc. Jpn.* **2003**, *72*, 2656.
(8) Han, W. Q.; Zettl, A. *J. Am. Chem. Soc.* **2003**, *125*, 2062.
(9) Prouhet, S.; Langlais, F.; Guette, A.; Naslain, R.; Rey, J. *Euro. J. Solid State Inorg. Chem.* **1993**, *30*, 953.
(10) Tang, C.; Bando, Y.; Sato, T.; Kurashima, K. *Chem. Commun.* **2002**, 1290.
(11) Pouchert C. J. *The Aldrich Library of FT-IR Spectra*; Aldrich Chemical Co.: Milwaukee, WI, 1985.
(12) Tang, C. C.; Bando, Y.; Ding, X. X.; Qi, S. R.; Golberg, D. *J. Am. Chem. Soc.* **2002**, *124*, 14550.

JA042388U

Supporting Information for

Fluorination and electrical conductivity of BN nanotubes

Chengchun Tang,*[a] Yoshio Bando,[a] Yang Huang,[b] Shuanglin Yue, [b] Changzhi Gu,[b] FangFang Xu, [a,c] and Dmitri Golberg [a]

[a] *Advanced Materials Laboratory, National Institute for Materials Science, Namiki 1-1, Tsukuba, Ibaraki 305-0044, Japan, and* [b] *Beijing National Laboratory for Condensed Matter Physics, Institute of Physics, Chinese Academy of Sciences, Beijing 100080, P. R. China, and Shanghai Ceramic Institute, Shanghai 200050, P. R. China*

Table of Contents:

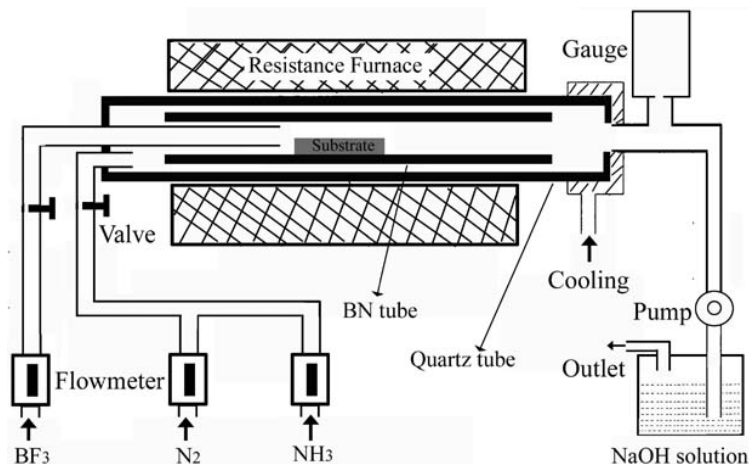**Experimental description and growth mechanism discussion**

Fiugre 3: Schematic diagram of experimental setup for the synthesis of F-doped BN nanotubes.

Experiment setup: The CVD reactor used in this study is shown in Figure 3. A BN tube was inserted into a quartz tube held in a standard resistance furnace. The furnace was first heated to reach 925°C in 30 mins in the nitrogen flow at a rate of 800 mL/min. Subsequently, the nitrogen flow was shut off and NH_3 and BF_3 gases were then simultaneously introduced at the flow rate of 1000 mL/min and 100 mL/min, respectively, and initiate the reaction. BF_3 gas was directly transported close to a substrate placed at reaction zone in order to prevent possible earlier reaction with NH_3, which may form solid ammonium fluoride to block the whole reaction system.

Caution: BF_3 is a highly toxic, colorless gas which fumes in a moist air. It can also react with a quartz tube. Therefore, during the reaction, the flow rate of ammonia must be large enough to react fully with BF_3. Care should also be taken to ensure that the reactor tube is never blocked. The exhausting gas should be fed through a water or NaOH solution bath cooling traps system to collect the remnant toxic gas.

Substrate Choice for F-doped BN nanotubes and growth mechanism: Although the reaction system described above is almost the same as a traditional CVD system that is used for the synthesis of BN films, our partial attention has been paid to the substrate choice. In order to check up the reaction system, we first used alumina and graphite substrate, and only BN crystalline particles were observed. Some chlorides such as $PbCl_2$ and $CaCl_2$ were also considered, a mixture of BN and fluoride particles was found. However, a tube-like product could be obtained when Mg- or transition metal-containing substrates were used. So far, we have tested Mg, Mg_3N_2, $MgCl_2$, MgF_2, nanosized Fe or Co and their oxides, etc. Except for $MgCl_2$, according to our experiments, no or ignorable amount of F atoms could be incorporated into BN nanotubes. However, when a piece of $MgCl_2$ lump was placed to the high temperature zone, colorless

fluorinated BN nanotubes of wool-like appearance fully covered the surface of the lump, and can be collected easily.

The mechanism of the nanotube formation may be properly understood because transition metals are commonly used as the catalysts for the one-dimensional material growth. Our previous experiments also indicated that Mg could promote the formation of BN nanotubes. However, some difficulties exist with respect to the understanding fluorination process. Taking into account that the excess in NH_4F or HF gases may fully destroy the as-generated nanotubes at a high temperature, based on the reaction,

$$BN + 3HF \rightarrow BF_3 + NH_3 \tag{3}$$

the local HF concentration near to the reaction zone must be appropriately adjusted so that the fluorination can be smoothly performed whereas the basic BN nanotube morphology is kept. Although the actual fluorination process is yet clear, we believe that the usage of $MgCl_2$ substrate is helpful for the control of HF concentration in the vicinity of lump surface due to the formation of a stable magnesium fluoride:

$$2F^- + MgCl_2 \rightarrow MgF_2 + 2Cl^- \tag{4}$$

Caution: The CVD reaction system must be fully isolated from the quartz tube supporting the BN chamber, because HF generated during the reaction can strongly erode the SiO_2 to form SiF_4 and H_2O. The existence of the H_2O vapor readily causes the contamination by SiO_x or $MgSiO_x$ solid solutions, or even prevents the F doping.

Fabrication of 4-probe measurement system: The fabrication process for patterning electrodes involves the following steps: 1) nanotubes were ultrasonically dispersed in ethanol and placed on a SiO_2/Si substrate; 2) Pt alignment marks are patterned using a focused ion beam system on the substrate for the positioning of an individual nanotube; 3) Electron Beam Lithography was applied to form the electrode patterns. 4) Au (50nm)/Ti (30nm) were sputtered onto the sample using a RF magnetron sputtering system and the process of lift-off was performed to form the device drawings. 5) A post-annealing process was adopted to obtain an improved Ohmic contact between the electrodes and nanotube. Electrical connection between the device drawings and the sample holder was made by an Ultrasonic Wire Bonder. The resistance and I-V curves of the individual nanotubes were measured by using a 220-grogrammable current source and a 181-nanovoltmeter (Keithley).
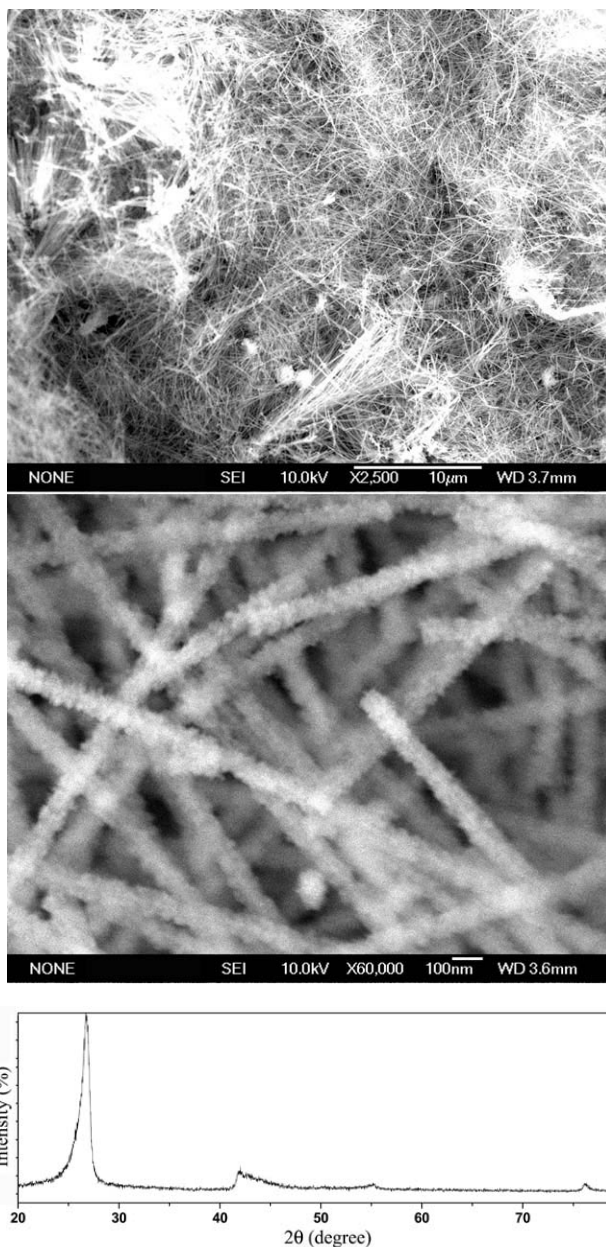
Figure 4. Scanning electron microscopy (SEM, JEOL 6300F) images and XRD pattern of the fluorine-functionalized BN nanotubes. The examinations by SEM reveal the one-dimensional structures with a markedly rough surface. The wall shells are considerably disordered. The nanotubes have high aspect ratios: the lengths of up to several micrometers and diameters of a few tens of nanometers. As established from the XRD pattern, the product contains pure BN crystals with the interlayer distance of ~0.33 nm.
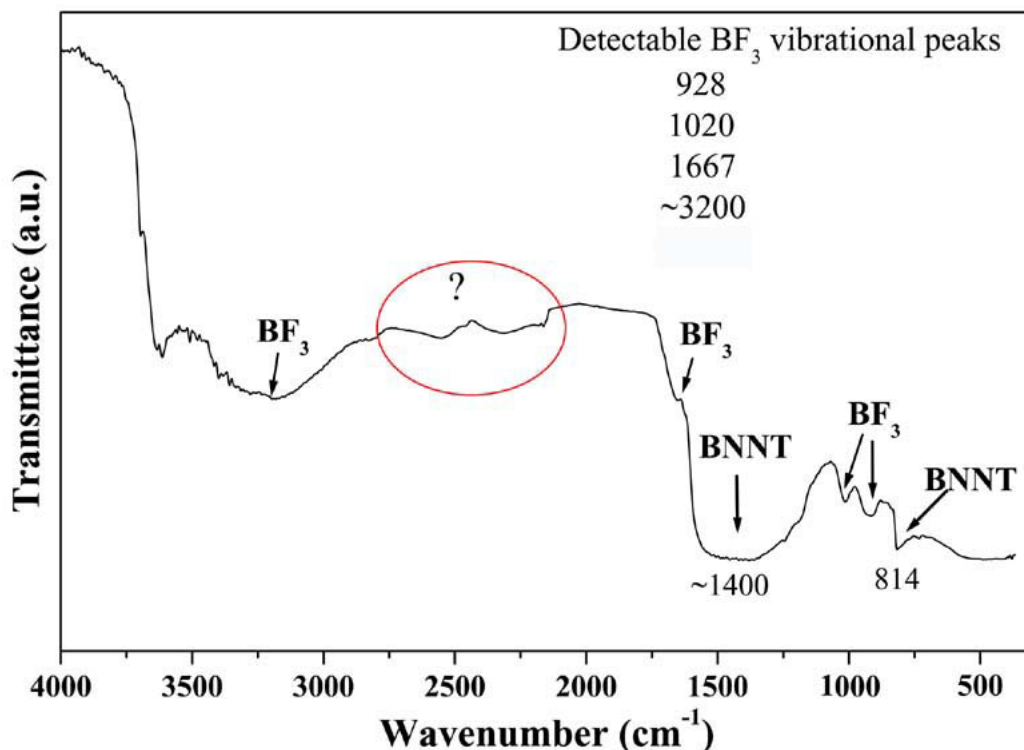
Figure 5. Fourier transformation infrared (FTIR, Shimadzu IR-400 spectrometer) spectrum of the fluorine-functionalized BN nanotubes. The spectrum shows a sharp absorption peak centered at approximately 810 cm^{-1}, which can be attributed to the B-N-B out-of-plane bending vibration perpendicular to the tube axis. The in-plane B-N transverse optical mode of BN nanotubes shows a broad absorption peak centered at ~1400 cm^{-1} with half-peak width of ~430 cm^{-1}, indicating a highly disordered atom arrangement along the tube axis. The primary vibrational features of covalent B-F bonds could also be detected from the spectrum, which approximately located at 930, 1020, 1240, 1670 and a broad peak near 3200 cm^{-1}. Although some peaks with relatively weak intensity (marked with a circle in the pattern) have not yet been assigned, the FTIR measurement clearly indicates the presence of F-doped BN nanotubes.

Figure 6. High-resolution transmission electron microscopy (TEM, JEM-3000F) image of fluorine-functionalized BN nanotubes, showing highly- disordered layers. The selected area electron diffraction pattern (inset) taken from an individual nanotube exhibits the spots from {002} and {110} diffractions spreading over the angles of ~45°. This further confirms the marked disordering within the BN tubular shells.
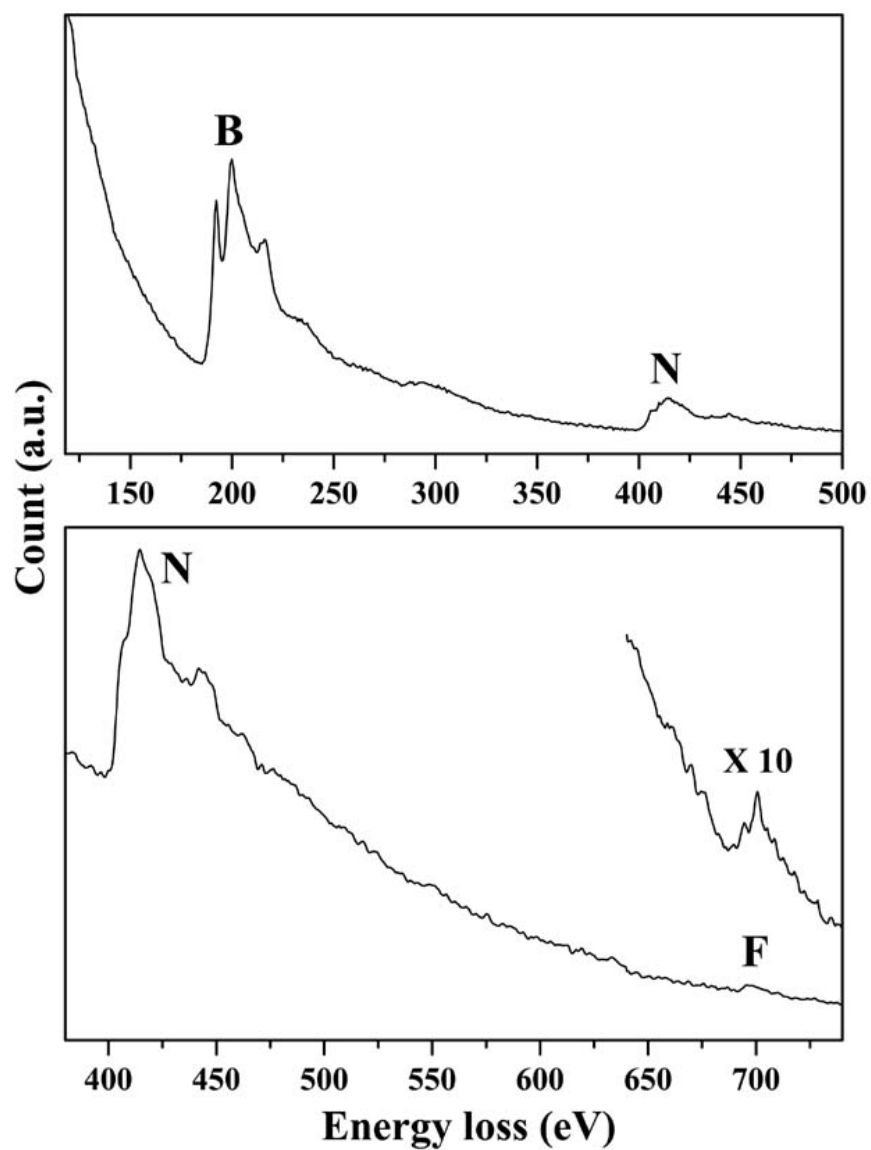
Figure 7. Electron energy loss (EEL) spectrum of the fluorine-functionalized BN nanotubes. B, N and F characteristic edges can be easily found. The N/B ratio calculated from this pattern is close to 1. F content relative to N, based on the pattern, is calculated as ~4.2 at %.
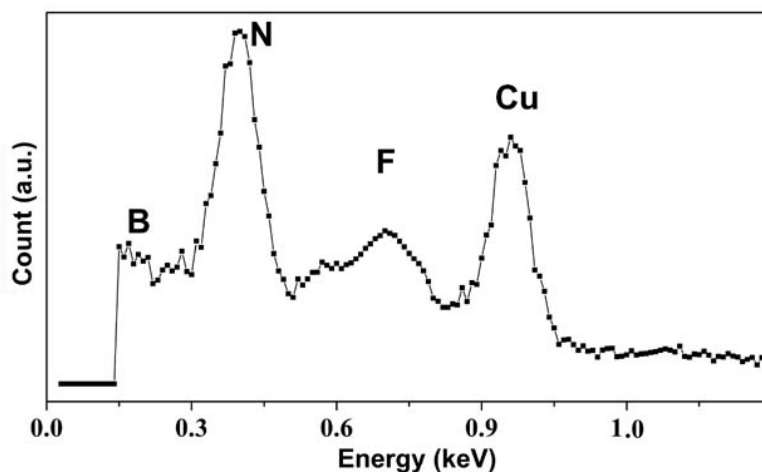
Figure 8. Energy-dispersive X-ray (EDX) spectrum of the fluorine-functionalized BN nanotubes, B, N and F signals could be found. The copper peak results from the TEM grid. The calculated concentration ratio is B:N:F = 1:0.97:0.07. (EDS system is not a sensitive technique to define the B content. Our EDX system has an onset energy value of ~0.15 keV which is close to the 0.19 keV of B peak, which makes the measurement of B peak area difficult. The definition of B/N ratio reported here is based on the reference to the EDX spectrum of pure BN nanotubes. Briefly, the relative area ratio of a B peak between 0.15 and 0.23 keV to a well-defined N peak is used as the standard area ratio for pure stoichiometric BN nanotubes. The B/N composition ratio of the current F-doped BN nanotubes are then calculated based on the standard peak ratio reference. Of course, the value obtained in this means is an approximation. The relatively accurate B/N ratio must be obtained from EELS technique, as shown in Figure 7. By contrast, a F content calculated using EDX measurement is more accurate than that obtained during EELS.)